Nitric Oxide 53 (2016) 13–21

Contents lists available at ScienceDirect

Nitric Oxide

journal homepage: www.elsevier.com/locate/yniox

Active site cysteine-null glyceraldehyde-3-phosphate dehydrogenase (GAPDH) rescues nitric oxide-induced cell death

Takeya Kubo [a], Hidemitsu Nakajima [a, *], Masatoshi Nakatsuji [b], Masanori Itakura [a], Akihiro Kaneshige [a], Yasu-Taka Azuma [a], Takashi Inui [b], Tadayoshi Takeuchi [a]

[a] Laboratory of Veterinary Pharmacology, Graduate School of Life and Environmental Sciences, Osaka Prefecture University, 1-58, Rinkuourai-kita, Izumisano, Osaka 5988531, Japan
[b] Laboratory of Biological Macromolecules, Graduate School of Life and Environmental Sciences, Osaka Prefecture University, 1-1, Gakuen-cho, Sakai, Osaka 5998531, Japan

ARTICLE INFO

Article history:
Received 28 August 2015
Received in revised form
30 November 2015
Accepted 23 December 2015
Available online 25 December 2015

Keywords:
GAPDH
Nitric oxide
Protein aggregation
Dominant-negative
Therapeutics

ABSTRACT

Glyceraldehyde-3-phosphate dehydrogenase (GAPDH), a homotetrameric enzyme involved in a key step of glycolysis, also has a role in mediating cell death under nitrosative stress. Our previous reports suggest that nitric oxide-induced intramolecular disulfide-bonding GAPDH aggregation, which occurs through oxidation of the active site cysteine (Cys-152), participates in a mechanism to account for nitric oxide-induced death signaling in some neurodegenerative/neuropsychiatric disorders. Here, we demonstrate a rescue strategy for nitric oxide-induced cell death accompanied by GAPDH aggregation in a mutant with a substitution of Cys-152 to alanine (C152A-GAPDH). Pre-incubation of purified wild-type GAPDH with C152A-GAPDH under exposure to nitric oxide inhibited wild-type GAPDH aggregation in a concentration-dependent manner *in vitro*. Several lines of structural analysis revealed that C152A-GAPDH extensively interfered with nitric oxide-induced GAPDH-amyloidogenesis. Overexpression of doxycycline-inducible C152A-GAPDH in SH-SY5Y neuroblastoma significantly rescued nitric oxide-induced death, concomitant with the decreased formation of GAPDH aggregates. Further, both co-immunoprecipitation assays and simulation models revealed a heterotetramer composed of one dimer each of wild-type GAPDH and C152A-GAPDH. These results suggest that the C152A-GAPDH mutant acts as a dominant-negative molecule against GAPDH aggregation via the formation of this GAPDH hetero-tetramer. This study may contribute to a new therapeutic approach utilizing C152A-GAPDH against brain damage in nitrosative stress-related disorders.

1. Introduction

In addition to its role in glycolysis, glyceraldehyde-3-phosphate dehydrogenase (GAPDH) is a multifunctional enzyme that is also involved in nitrosative stress-induced cell death [1]. There are two main pathways of GAPDH-mediated cell death [2]. First, GAPDH nuclear translocation under conditions of nitrosative stress such as a nitric oxide donor s-nirosoglutathione promotes the expression of several apoptosis-related genes such as p53 upregulated modulator of apoptosis (PUMA) and Bcl2-associated X protein (BAX) [3,4]. Second, GAPDH aggregation induced by oxidative/nitrosative stress is likely to trigger cellular dysfunction accompanied with energy depletion both *in vitro* and *in vivo* [5–7].

In several neurological disorders that occur under oxidative/nitrosative stress in the brain, the accumulation of protein aggregation and the subsequent increase in aberrant aggregates promote the formation of pathological deposits (usually termed amyloids), leading to the causality of these diseases [8]. Some reports indicate that insoluble GAPDH aggregation occurs in pathological amyloidal deposits, including senile plaques and neurofibrillary tangles in Alzheimer's disease [9], and Lewy bodies in Parkinson's disease [10]. Further, massive production of nitric oxide in the brain is likely to play a critical role in the pathogenesis [11,12]. From these

Abbreviations: ADH, alcohol dehydrogenase; AFM, atomic force microscopy; ALD, aldolase; DOX, doxycycline; GAPDH, glyceraldehyde-3-phosphate dehydrogenase; GSH, glutathione; MDH, malate dehydrogenase; Mw, molecular weight; NO, nitric oxide; NOC18, 1-hydroxy-2-oxo-3,3-bis(2-aminoethyl)-1-triazene; NOR3, (±)-(E)-4-ethyl-2-[(E)-hydroxyimino]-5-nitro-3-hexenamide; PBS, phosphate-buffered saline; PMSF, phenylmethylsulfonyl fluoride; WT, wild type.

* Corresponding author.
E-mail address: hnakajima@vet.osakafu-u.ac.jp (H. Nakajima).

http://dx.doi.org/10.1016/j.niox.2015.12.005

observations, we previously discovered that the active site cysteine (Cys-152) plays an essential role in nitric oxide-induced disulfide-bonding amyloid-like GAPDH aggregation: a mutant with a substitution of Cys-152 to alanine (C152A-GAPDH) fails to aggregate even in the presence of nitrosative stress [5–7]. Additionally, it has been reported that GAPDH is structurally altered in association with nitrosative stress in brain damage [13,14]. Thus, abnormal changes in GAPDH structure seem to play a critical role in the pathogenesis of these diseases related to excessive emergence of nitric oxide [15].

A high-resolution structure of human GAPDH has been published [16]. Human GAPDH is an asymmetric homotetramer consisting of a dimer of dimers with specific dimerization domains [16,17]. Also, heteromeric hybridization can easily occur among dimers of GAPDH derived from various species [18,19]. Further, the oligomeric status of the GAPDH-C152A mutant is completely similar to that of wild-type GAPDH [7]: GAPDH exists as an equilibrium mixture of tetramers, dimers, and monomers [20]. These findings lead us to hypothesize that C152A-GAPDH might be able to interfere with wild-type GAPDH aggregation induced by nitric oxide and might therefore provide a novel therapeutic for nitric oxide induced-GAPDH aggregation-related neurodegenerative/neuropsychiatric disorders.

Here, we report that C152A-GAPDH acts as a dominant-negative mutant protecting against GAPDH aggregation-induced cell death in SH-SY5Y neuroblastoma under nitrosative stress, through the formation of a heterotetramer between wild-type GAPDH and C152A-GAPDH. The therapeutic implications utilizing this mutant *in vivo* are discussed.

2. Materials and methods

2.1. Chemicals, antibodies, and plasmids

Unless otherwise noted, chemicals were of analytical grade. Mouse anti-GAPDH monoclonal antibody (MAB374) was obtained from Millipore Japan (Tokyo, Japan); rabbit anti-GAPDH polyclonal antibody (ab9485) was obtained from Abcam (Cambridge, MA); rabbit polyclonal anti-Myc antibody (A-14: sc-789) and rabbit polyclonal anti-His antibody (Omni-probe, M-21: sc-499) were obtained from Santa Cruz Biotechnology (Santa Cruz, CA); mouse anti- β-actin monoclonal antibody was obtained from Sigma–Aldrich Japan (Tokyo, Japan). Human wild type- (WT-) *GAPDH* cDNA was generated as reported previously [7]. For bacterial expression, cDNA was cloned into pBAD-HisA (Invitrogen, Carlsbad, CA) using the SacI-KpnI sites. For mammalian cell line expression, the cDNA was cloned into pcDNA4-TO-Myc/HisA (Invitrogen) using the EcoRI-EcoRV sites. The alanine-substituted mutant C152A-GAPDH was generated using the QuikChange site-directed mutagenesis kit with WT-GAPDH as the template, according to the manufacturer's protocol (Stratagene, La Jolla, CA), as reported previously [7].

2.2. Expression and purification of recombinant GAPDH

The pBAD-HisA vector carrying WT- or C152A-GAPDH cDNA was transformed into gap (−) *Escherichia coli* strain W3CG [21]. Expression and purification of these recombinant GAPDH proteins were carried out as described previously [5,7]. Protein concentrations were determined spectrophotometrically assuming a ε0.1% of 1.0 at 280 nm.

2.3. In vitro aggregation assay

The *in vitro* aggregation assay for purified proteins was performed basically according to published methods [5,7]. Purified His-tagged WT-GAPDH (0.3 mg/ml) with His-tagged C152A-GAPDH (0.3, 0.5, or 0.75 mg/ml) were mixed with or without pre-incubation for 24 h at 4 °C, and then the mixtures were treated with 100 μM NOR3 (a NO generator, DOJINDO, Kumamoto, Japan) for 24 h at 37 °C. To measure the turbidity of the solutions, the absorbance at 405 nm was recorded using a VERSA Max microplate reader (Molecular Devices Japan, Tokyo, Japan). Alternatively, the turbidities of purified His-tagged WT-GAPDH (0.3 mg/ml) with alcohol dehydrogenase (ADH, 0.83 mg/ml, Sigma–Aldrich Japan, Tokyo, Japan), malate dehydrogenase (MDH, 0.69 mg/ml, Roche Diagnostics, Basel, Switzerland), or aldolase (ALD, 0.79 mg/ml, Roche Diagnostics) were measured as a same condition as the assay using C152A-GAPDH (0.75 mg/ml). The each gram concentration of ADH (Mw = 40 kDa), MDH (Mw = 33 kDa), or ALD (Mw = 38 kDa) was determined as equal to the same molar concentration of C152A-GAPDH (Mw = 36 kDa). The turbidities of purified His-tagged WT-GAPDH (0.3 mg/ml) with glyceraldehyde-3-phosphate (GAP, 2 mM) or glutathione (GSH, 1, 3, or 10 mM) were measured as described above.

2.4. In vitro GAPDH hybridization

Purified erythrocyte human GAPDH (0.3 mg/ml, Sigma–Aldrich Japan) and His-tagged C152A-GAPDH (0.3, 0.6, or 0.75 mg/ml) were mixed and incubated in G2′ buffer containing 50 mM Tris–HCl (pH = 8.0), 150 mM NaCl, 1 mM EDTA, and 5% glycerol for 24 h at 4 °C. Then, samples (500 μl) were subjected to an *in vitro* immunoprecipitation assay using both anti-His polyclonal antibody (1 μg/assay) and protein-G sepharose (GE Healthcare Japan, Tokyo, Japan) according to published biochemical protocols [22]. Hybridization between native GAPDH and His-tagged recombinant GAPDH was analyzed by 5–20% SDS-PAGE, and each protein was stained with 0.5% (w/v) Coomassie brilliant blue. The intensity of the bands was measured using Scion image software ver. 4.0.3.2. (Scion Corporation, Frederick, MD).

2.5. Analyses of amyloid-like aggregation of GAPDH

Purified WT-GAPDH (0.3 mg/ml) without or with C152A-GAPDH (0.75 mg/ml) was treated with NOR3 (100 μM) for 24 h, and subjected to following analyses. Thioflavin-T fluorescence: Seventy microliters of each sample mixture were added to 2 ml of Thioflavin-T solution (10 μM in 50 mM glycine buffer, pH 8.0, Sigma–Aldrich Japan), and the fluorescence intensities were measured at 450 nm excitation and 482 nm emission wavelengths using an F-2000 fluorescence spectrophotometer (Hitachi, Tokyo, Japan). Congo Red spectral: Congo Red (2.5 μM, Sigma–Aldrich Japan) was added to the mixture, and incubated for 30 min in the dark. Subsequently, the absorbance of mixtures (wavelength from 400 nm to 600 nm) was scanned using an U3210 spectrophotometer (Hitachi). Atomic Force Microscopy (AFM): The sample mixtures were spotted onto fresh cleaved mica, incubated for 1 min, rinsed three times with water, and then dried. All measurements were carried out in "tapping mode" under ambient conditions with single-beam silicon cantilever probes. Three regions of the mica surface were examined to ensure that an accurate sample of the structures on the mica was obtained [23].

2.6. Cell culture and biochemical analysis

Human neuroblastoma SH-SY5Y cells (American Type Culture Collection, ATCC, Manassas, VA) were grown in Dulbecco's modified Eagle medium/Ham's F12 Medium (DMEM/F12) supplemented with 10% fetal bovine serum, 2 mM glutamine, and antibiotics–antimycotics (Invitrogen) at 37 °C in a 5% CO_2 humidified

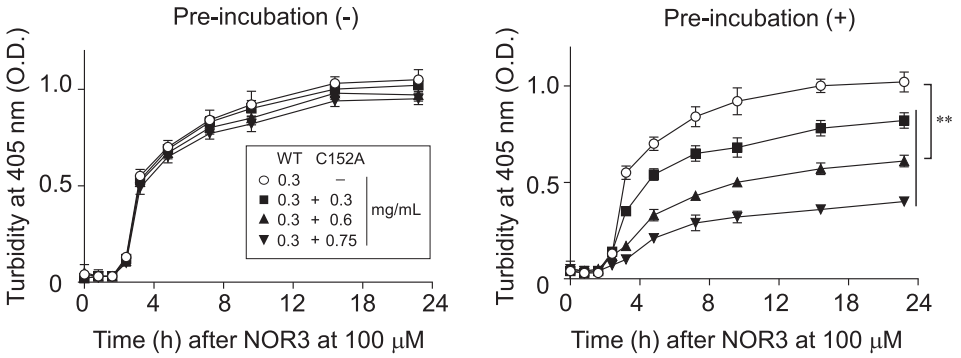

Fig. 1. C152A-GAPDH inhibits NO-induced GAPDH aggregation. The concentration-dependent effect of C152A-GAPDH on the formation of NOR3-induced GAPDH aggregates is shown. Mixtures of His-tagged WT-GAPDH (0.3 mg/ml) and C152A-GAPDH (0, 0.3, 0.5, or 0.75 mg/ml), without (left panel) or with (right panel) pre-incubation, were incubated at 37 °C for the indicated time periods with NOR3 (100 μM) treatment, and the turbidity of the solutions was measured in terms of absorbance at 405 nm. (n = 4, **, $p < 0.01$).

incubator. The generation of stable cell lines for the inducible expression of GAPDH has been established as reported previously [7]. Subcellular fractionation was carried out according to the following procedures. After 48-h treatment with either control vehicle (0.1 N NaOH) or a NO generator NOC18 (DOJINDO), cells were washed twice with phosphate-buffered saline (PBS) and then incubated for 5 min in ice-cold PBS containing 40 mM iodoacetamide to protect unmodified thiols from oxidation during fractionation. All subsequent steps were performed at 4 °C. Cells were scraped into 500 μl of buffer A containing 10 mM Tris–HCl (pH 7.5), 10 mM NaCl, 3 mM $MgCl_2$, 0.05% Nonidet P-40, 0.5% Triton-X100, 40 mM iodoacetamide, 1 mM phenylmethylsulfonyl fluoride (PMSF), and protease inhibitor mixture (Roche Diagnostics). After 30 min, the cell suspension was homogenized vigorously for 15 s with rocking. The total lysate was centrifuged at 20400 × *g* for 10 min, and the pellet was collected to prepare the insoluble fraction. To assess GAPDH hybridization in cells, the purified lysates were subjected to an immunoprecipitation assay using both anti-

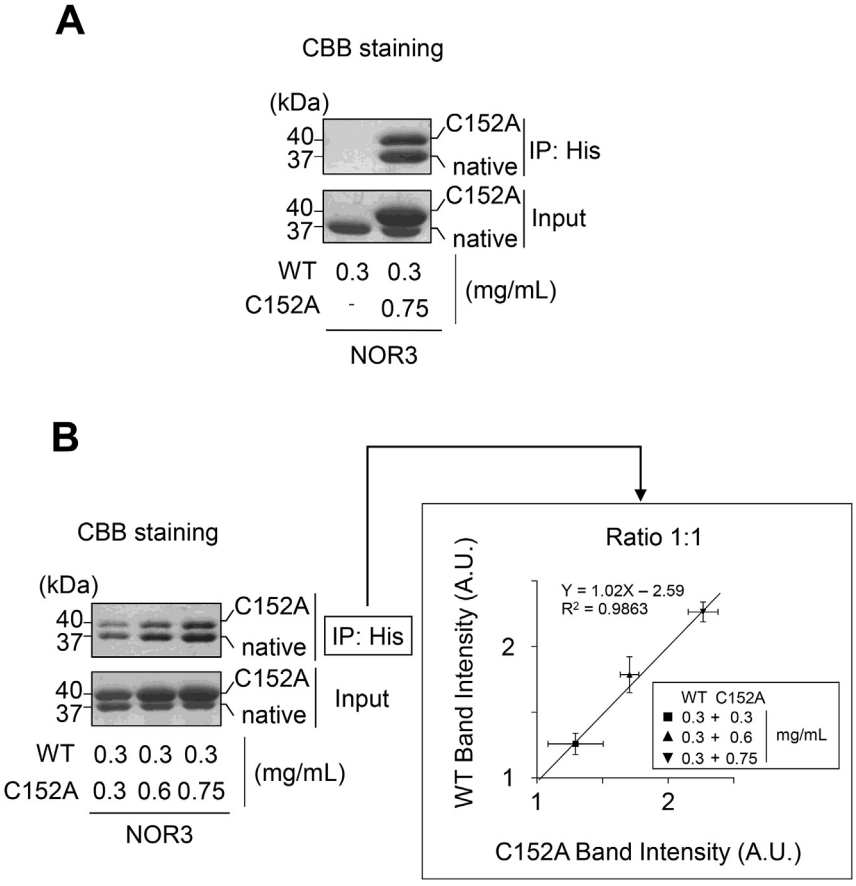

Fig. 2. C152A-GAPDH hybridizes with WT-GAPDH. (A) Hybrid formation of native (corresponding to WT-GAPDH) and His-tagged C152A-GAPDH is shown. Purified human native GAPDH (0.3 mg/mL) and C152A-GAPDH (0 or 0.75 mg/mL) were mixed and incubated at 4 °C for 24 h. These solutions were immunoprecipitated with anti-His polyclonal antibody, and subjected to 5–20% SDS-PAGE (n = 3). (B) The stoichiometry of hybrid formation between WT-GAPDH (native form, 0.3 mg/ml) and C152A-GAPDH (0.3, 0.6, or 0.75 mg/ml) is shown (n = 4). The regression line and correlation coefficient (R^2) in right panel are calculated by GraphPad Prism.

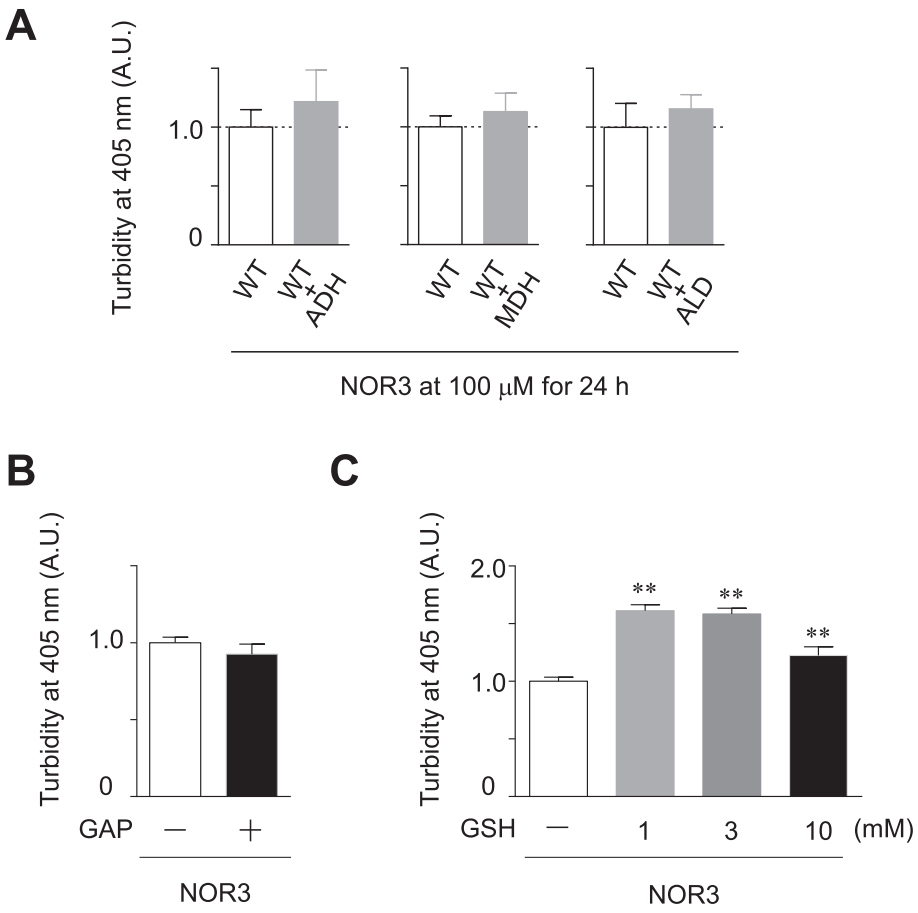

Fig. 3. Effects of other cysteine-containing glycolytic enzymes, glyceraldehyde-3-phosphate (GAP), or glutathione (GSH) on NO-induced GAPDH aggregation. (A) The effect of alcohol dehydrogenase (ADH), malate dehydrogenase (MDH), or aldolase (ALD) on NOR3-induced GAPDH aggregate formation is shown. Mixtures of WT-GAPDH (0.3 mg/mL) and ADH (0 or 0.83 mg/mL), MDH (0 or 0.69 mg/mL), or ALD (0 or 0.79 mg/mL), were incubated at 37 °C for 24 h under NOR3 (100 μM) treatment, and the turbidity of these solutions was measured in terms of absorbance at 405 nm (n = 4). (B) The effect of GAP at 2 mM on NOR3-induced GAPDH aggregate formation is shown. (n = 4) (C) The effect of GSH at 1, 3, or 10 mM on NOR3-induced GAPDH aggregate formation is shown. (n = 4, **, $p < 0.01$).

Myc polyclonal antibody (1 μg/assay) and protein-G sepharose (GE Healthcare Japan, Tokyo, Japan) according to published biochemical protocols [22]. The ratio of hybrid GAPDH molecule between endogenous and Myc-tagged wild-type/C152-GAPDH was calculated based on band intensities obtained via Western blotting, using the anti-GAPDH monoclonal antibody. Detection was performed using both SuperSignal West Pico Chemiluminescent Substrate and HyperFilm according to the manufacturer's procedure (GE Healthcare Japan). The band intensities were measured using Scion imaging software. To detect insoluble GAPDH oligomers in cells, the pellet obtained from the total cell lysate was then resuspended in 200 μl of buffer B containing 10 mM HEPES-KOH (pH 7.4), 25 mM NaCl, 3 mM $MgCl_2$, 300 mM sucrose, 40 mM iodoacetamide, 1 mM PMSF, and protease inhibitor mixture (Roche Diagnostics), and washed 3 times by centrifugation (3000 × *g* for 10 min), followed by suspension in buffer. After the addition of 100 μl of buffer B, the pellet was sonicated for 30 s and finally obtained as the insoluble fraction. These fractions were stored at −80 °C until use. Protein concentrations of the samples were determined by the Bradford assay (Bio-Rad Laboratories, Hercules, CA). Both total lysates and fractionated proteins were mixed with low SDS-sample buffer (final concentration: 62.5 mM Tris–HCl [pH 6.8], 0.5% SDS, 10% glycerol, 0.002% bromophenol blue) and then heated at 100 °C for 5 min. These samples were separated by 5–20% non-reducing SDS-PAGE and transferred to a nitrocellulose membrane (Bio-Rad Laboratories). The membranes were incubated for 1 h with Blocking One (Nacalai Tesque, Kyoto, Japan) to block nonspecific binding. The membrane was then incubated for 2 h at room temperature with an anti-GAPDH monoclonal antibody (1:300) or an anti-β-actin monoclonal antibody (1:4000) in 10% Blocking One-PBST (0.05% Tween 20, and 0.02% NaN_3 in PBS), followed by incubation for 1 h at room temperature with peroxidase-conjugated affinity-purified secondary antibody (Invitrogen). Detection of insoluble GAPDH oligomers was performed using both SuperSignal West Pico Chemiluminescent Substrate (GE Healthcare Japan) and LAS3000 (FUJI-FILM, Tokyo, Japan). The intensity of the bands was measured using Multi Gauge V3.0 (FUJI-FILM).

2.7. Cell immunofluorescence

We performed immunofluorescence as described previously [6,7]. The cells were then incubated overnight at 4 °C with an anti-GAPDH polyclonal antibody (1:1000) in 10% Blocking One-PBST. After washing four times with PBST, specific signals were visualized by staining the cells with an Alexa568-conjugated secondary antibody (1:2000, Invitrogen) using a confocal scanning microscope (C1si-TE2000-E; Nikon, Tokyo, Japan). For semi-quantification of cells with aggregates, five microscopic fields were selected at random, and the number of cells with aggregates among at least 500 total cells was quantified as a percentage [7].

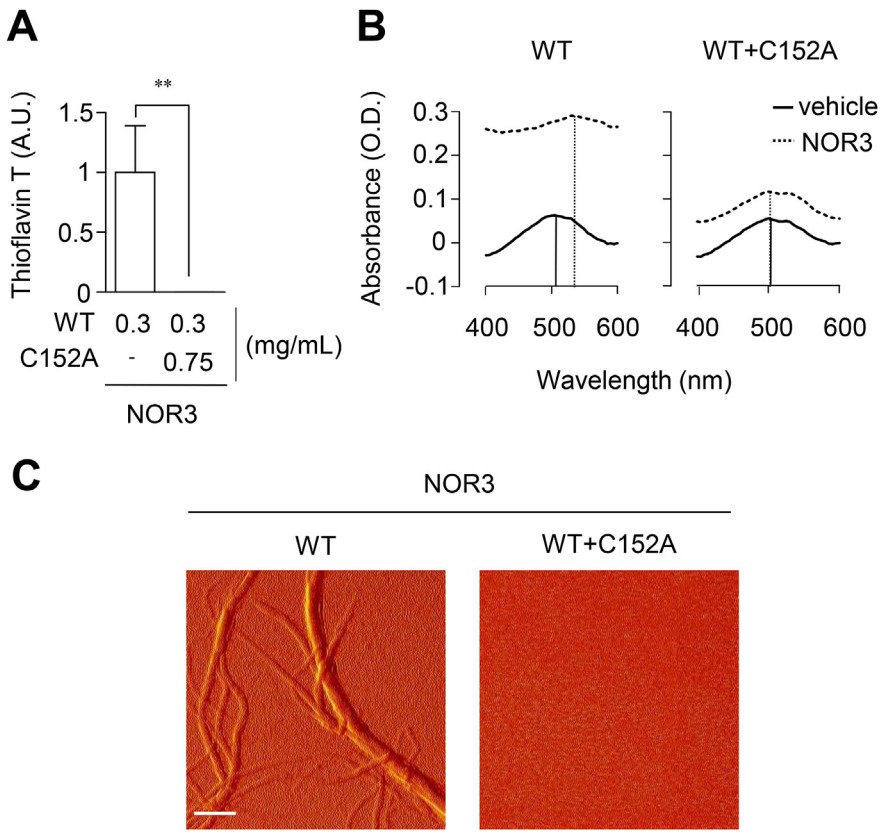

Fig. 4. C152A-GAPDH inhibits NO-induced GAPDH amyloidogenesis. (A) The effect of C152A-GAPDH (0.75 mg/ml) on NOR3 (100 μM for 24 h at 37 °C)-induced amyloid formation by WT-GAPDH (0.3 mg/ml) is shown. Thioflavin-T binding-dependent fluorescence of recombinant GAPDH treated with NOR3 is shown (n = 3, **, $p < 0.01$). (B) The absorbance spectra of Congo Red are shown. WT- and C152A-GAPDH were mixed and treated with NOR3. After incubation, Congo Red solution was added, and the absorbance of the final solution was measured. (C) Morphological analysis of recombinant GAPDH mixtures (WT and WT plus C152A) treated with NOR3 by AFM is shown. Scale bar = 0.5 μm.

2.8. Cell viability

Cytotoxicity was measured in terms of cell viability using the Cell Titer Glo Luminescent Cell Viability Assay kit (Promega, Madison, WI) according to the manufacturer's protocol [7].

2.9. Docking simulation of GAPDH heterotetramer composed of a dimer of wild-type and a dimer of C152A-GAPDH

Structural model of a GAPDH heterotetramer, formed from a dimer of human wild-type GAPDH (PDB code 1U8F) and a dimer of C152A-GAPDH, generated by ZDOCK version 3.0.2 [24].

2.10. Statistical analysis

All data represent the mean ± S.D. of independent experiments, with the number of repeats (n) indicated in each Figure legend. For statistical analysis, two groups and multiple groups were compared using the unpaired Student's t test or Dunnet's multiple test after one-way analysis of variance (ANOVA), respectively (GraphPad Prism ver. 6.01, GraphPad Software, Inc., CA).

3. Results and discussion

We previously reported that the C152A-GAPDH mutant, which contained an alanine substituted at the site of the active site cysteine residue responsible for GAPDH aggregation, lacked its aggregation property under oxidative/nitrosative stress conditions [7]. Therefore, we first tested how C152A-GAPDH influences nitric oxide (NO)-induced wild-type (WT)-GAPDH aggregation *in vitro* (Fig. 1). Treatment of His-tagged WT-GAPDH (0.3 mg/ml) with NOR3, a NO generator, resulted in an increase in the turbidity of the solution, *i.e.*, GAPDH aggregation (Fig. 1, white circles). Pre-incubation of WT-GAPDH with C152A-GAPDH (0.3, 0.6, or 0.75 mg/ml) ameliorated NOR3-induced WT-GAPDH aggregation in a concentration-dependent manner (Fig. 1, right panel, black symbols). This inhibitory effect was seen only following pre-incubation of these mixtures (Fig. 1, right panel), indicating the conversion of the oligomeric status of the WT-/C152A-GAPDH tetramer, dimer, and monomer at equilibrium. These results suggest hybridization between WT-GAPDH and C152A-GAPDH. GAPDH variants derived from different species easily form hybrid tetramers [18]. Therefore, we confirmed whether native GAPDH (corresponding to WT-GAPDH) is able to hybridize His-tagged C152A-GAPDH by an immunoprecipitation assay using an anti-His antibody (Fig. 2). Under conditions of pre-incubation of native GAPDH (0.3 mg/ml) with His-tagged C152A-GAPDH (0.75 mg/ml), native GAPDH was co-immunoprecipitated with His-tagged C152A-GAPDH (Fig. 2A), indicating that each WT-GAPDH molecule within tetramer can hybridize with C152A-GAPDH protein subunits. To further address the stoichiometry of hybridization between WT- and C152A-GAPDH, we performed the co-immunoprecipitation assay using WT-GAPDH (0.3 mg/ml) pre-incubated with different amounts of C152A-GAPDH (0.3, 0.6, or 0.75 mg/ml, Fig. 2B). The ratio of co-immunoprecipitated native GAPDH and His-tagged C152A-GAPD was approximately 1:1 in all of concentrations of C152A-GAPDH (Fig. 2B, right panel). Thus, C152A-GAPDH appears to interfere with NOR3-induced WT-GAPDH aggregation through

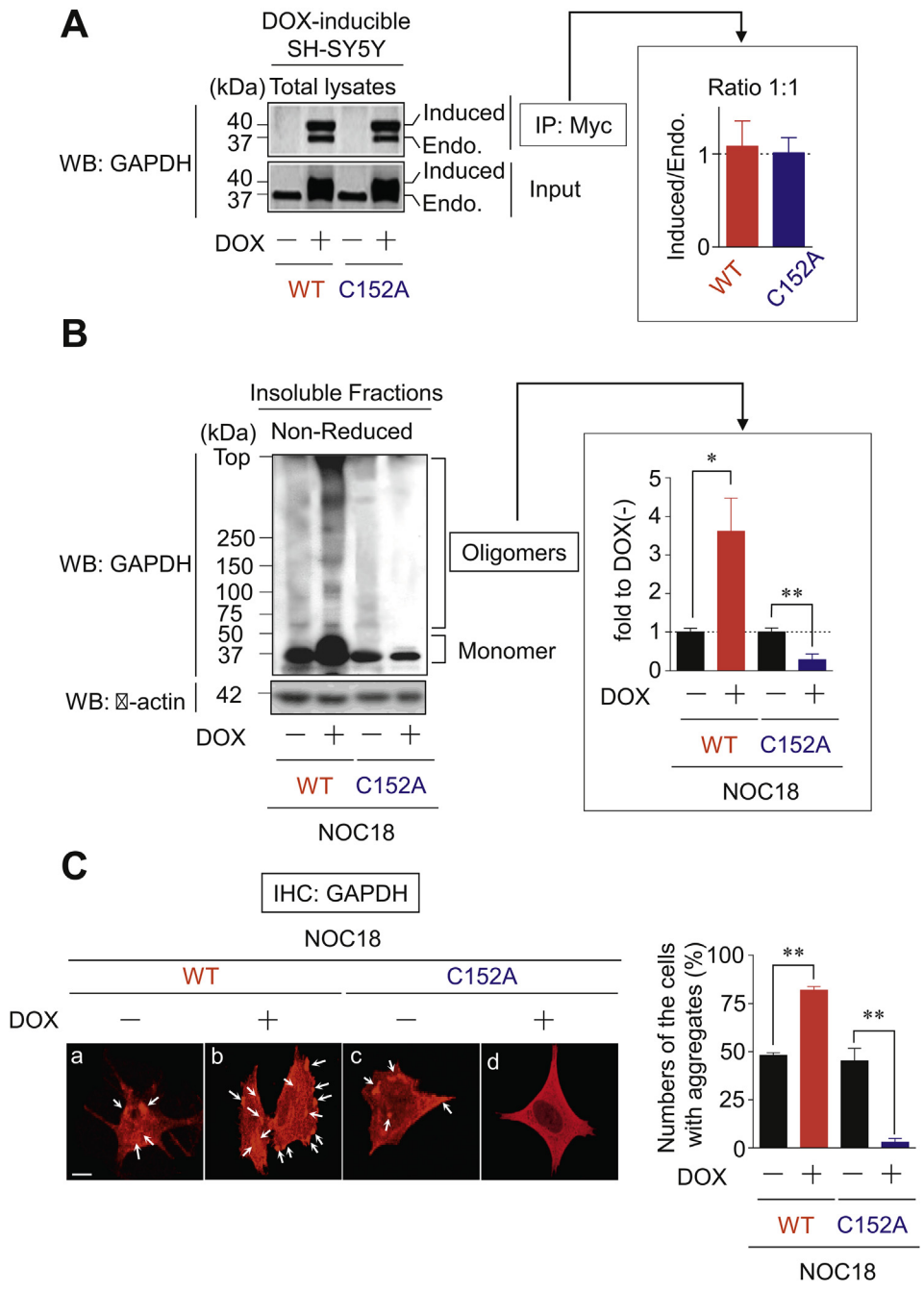

Fig. 5. Expression of C152A-GAPDH inhibits the formation of GAPDH aggregates in SH-SY5Y cells. (A) Hybrid formation of endogenous GAPDH and induced-GAPDH in doxycycline (DOX)-inducible GAPDH cells is shown. Bars indicate the ratio of induced/endogenous GAPDH (n = 3). (B) NOC18 (200 μM)-induced GAPDH aggregates in the insoluble fraction of DOX-inducible SH-SY5Y cells are shown. The bars indicate the semi-quantification of band intensities of the GAPDH aggregates (described as oligomers) (n = 3, *, $p < 0.05$; **, $p < 0.01$). The blots of β-actin are used for a loading control. (C) Fluorescence of total GAPDH (red) in WT- and C152A-GAPDH inducible cells without (−) or with (+) DOX treated with NOC18 (200 μM, 48 h) is shown. The arrows indicate GAPDH aggregates. The numbers of cells with GAPDH aggregates were measured (right panel, n = 5, **, $p < 0.01$). Scale bar = 10 μm.

the formation of the hybrid tetramer consisting of equal number of each subunit. Further, the addition of the same molar amount of other cysteine-containing glycolytic enzymes of alcohol dehydrogenase (ADH), malate dehydrogenase (MDH), or aldolase (ALD), which are lacking the property of NO-induced aggregation [5], did not inhibit GAPDH aggregation (Fig. 3A). We next investigated effect of its substrate glyceraldehyde-3-phosphate (GAP) on NO-induced GAPDH aggregation because GAP binds to Cys-152 to form a thiohemiacetal intermediate during the glycolytic reaction [20] (Fig. 3B). GAP did not affect NO-induced GAPDH aggregation (Fig. 3B). Further, high concentrations (1–10 mM) of glutathione (GSH), which are abundantly present in cells as an endogenous anti-oxidant, rather augmented NO-induced GAPDH aggregation (Fig. 3C). Together, these results suggest that the C152A-GAPDH molecule is a specific dominant-negative mutant against NO-induced GAPDH aggregation.

We next examined whether C152A-GAPDH affected the NO-induced amyloidal characteristics of WT-GAPDH aggregates (Fig. 4). Co-incubation of WT-GAPDH with C152A-GAPDH resulted in no fluorescence from the amyloid-binding dye Thioflavin-T

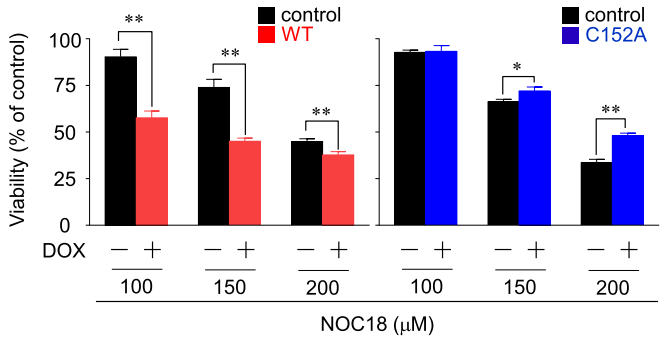

Fig. 6. NO-induced cell death is restored by C152A-GAPDH expression. Effect of 48-h incubation with NOC18 (100, 150, or 200 μM) on the cell viabilities of WT- (left panel) and C152A- (right panel) inducible cells without (−) or with (+) DOX treatment is shown (n = 3–4 *, p < 0.05, **, p < 0.01).

(Fig. 4A). Numerous amyloid proteins exhibit an inherent spectral shift upon incubation with an amyloid dye Congo Red from approximate 500 nm to about 540 nm [25]. Although treatment of NOR3 with WT-GAPDH consistently shifted the peak of the Congo Red spectrum from 505.2 nm to 530.4 nm (Fig. 4B, left panel), co-incubation with C152A-GAPDH inhibited the spectral shift even in the presence of NOR3 (wavelength of maximal fluorescence emission for WT-GAPDH = 499.8 nm, WT-GAPDH plus C152A-GAPDH = 500.4 nm; Fig. 4B, right panel). Moreover, morphological analysis using an atomic force microscope (AFM) revealed that fibril structure formation by WT-GAPDH was inhibited by the addition of C152A-GAPDH under NOR3-treatment (Fig. 4C). Thus, C152A-GAPDH is also likely to act as a specific dominant-negative mutant against the amyloid-like characteristics of NO-induced GAPDH aggregates.

To further investigate the dominant-negative effect of C152A-GAPDH in cells, we examined whether the overexpression of C152A-GAPDH in doxycycline (DOX)-inducible SH-SY5Y cells resulted in the formation of a hybrid with endogenous GAPDH. Similar to the results in Fig. 1, we confirmed that both Myc-tagged WT and C152A-GAPDH induced by Dox hybridized with endogenous GAPDH in cells in an immunoprecipitation assay using an anti-Myc antibody (Fig. 5A, left panel). The ratio of co-immunoprecipitated endogenous GAPDH and Myc-tagged WT/C152A-GAPDH was approximately 1:1 (Fig. 5A, right panel), similar to the results obtained from purified GAPDH (Fig. 2B). Then, Western blot analysis showed that the levels of DOX-induced plus endogenous aggregated GAPDH oligomers induced by NOC18 (a NO generator, 200 μM) in insoluble fractions were significantly augmented by WT-GAPDH overexpression (Fig. 5B). Consistently, the overexpression of C152A-GAPDH extensively ameliorated NOC18-induced endogenous GAPDH aggregation (Fig. 5B). Under these conditions, we assessed the levels of cells with total GAPDH aggregates, which were concomitant with the levels of insoluble GAPDH oligomers obtained from Western blot analysis (Fig. 5B). Similar results were assessed by a cell immunofluorescence analysis (Fig. 5C). These results support the *in vitro* study (Figs. 1 and 2), which showed that the presence of the C152A-GAPDH dominant-

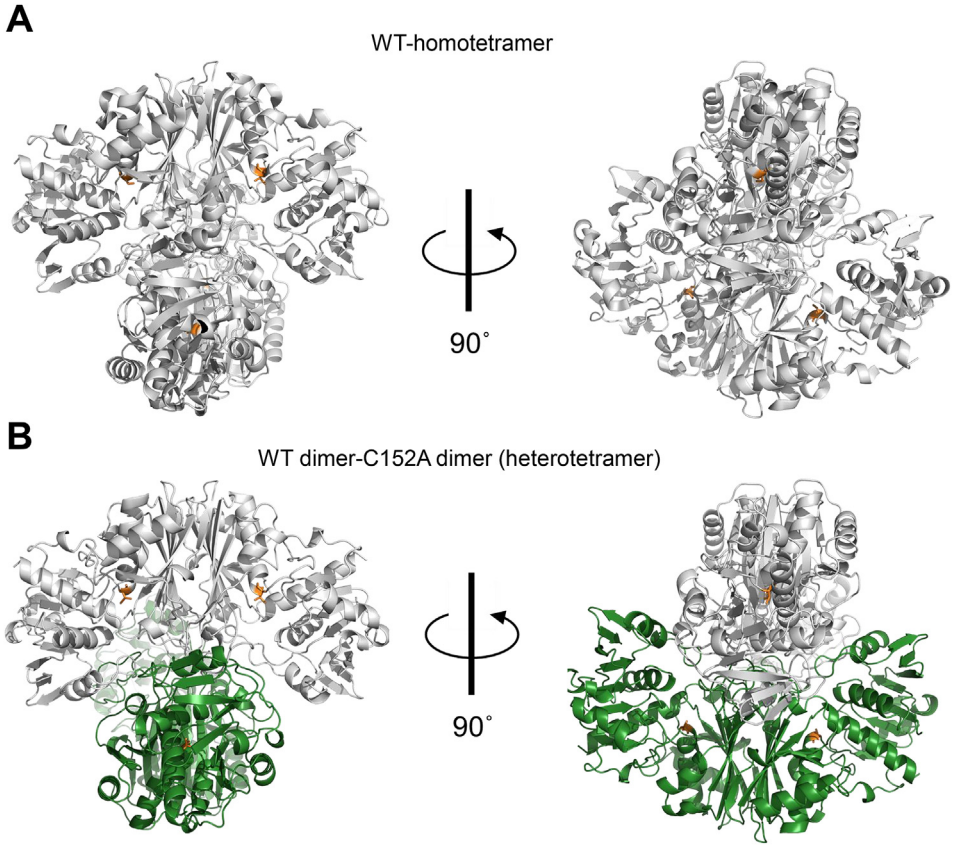

Fig. 7. Simulation of GAPDH-heterotetramer of the human WT-GAPDH dimer to a dimer of human C152A-GAPDH. (A) Structure of human GAPDH-homotetramer (PDB number: 1U8F) is shown. (B) A docking model of GAPDH-heterotetramer of the human WT-GAPDH dimer (silver) to a dimer of human C152A-GAPDH (green) is shown. The simulation was performed by ZDOCK Version 3.0.2. The active site Cysteine-152 in WT-GAPDH and Alanine-152 substituted for Cysteine in C152A-GAPDH are colored as orange.

negative mutant interferes with NO-induced GAPDH aggregation via the formation of a hybrid molecule with endogenous GAPDH.

To clarify the linkage between levels of GAPDH aggregation and NO-induced cell death, we investigated the effect of overexpression of WT- and C152A-GAPDH on NOC18-induced cell death (Fig. 6). In agreement with our previous findings using dopamine as an oxidative/nitrosative stressor [6,7], significant augmentation of cell death was observed in inducible cells overexpressing WT-GAPDH (Fig. 6, left panel). Conversely, prominent protection by overexpression of C152A-GAPDH was observed under NOC18-treatment (Fig. 6, right panel). Hence, NOC18-induced cell death is likely to correlate with the levels of GAPDH aggregation in each inducible cell, suggesting the disturbance of endogenous GAPDH aggregation by the formation of a hybrid molecule with C152A-GAPDH.

In the present study, we identified that C152A-GAPDH acts as a dominant-negative mutant against GAPDH aggregation and provides protection against cell death under exposure to nitrosative stress. We previously reported that the overexpression of C152A-GAPDH in SH-SY5Y has no-influence on cellular glycolytic activity [7]. In this context, we also found that NO-induced GAPDH aggregation in cells is not impacted by glucose concentrations in culture medium (data not shown); cellular event of GAPDH aggregates formation under nitrosative stress is not related to glycolysis. Thus, the dominant-negative effect of C152A-GAPDH is purely dependent on the formation of the hybrid GAPDH molecule, leading to interference of GAPDH aggregation-induced cell death. Human GAPDH is a homotetramer best described as a dimer of dimers (Fig. 7A) [16,17]. Also, heteromeric hybridization of GAPDH dimer, e.g., a heterotetramer derived from various monomeric species, is formed easily [18,19]. Indeed, immunoprecipitation assays in this study demonstrate the formation of hybrid GAPDH, consisting of native GAPDH and His-tagged recombinant WT-GAPDH, or cellular endogenous GAPDH and Myc-tagged recombinant WT-/C152A-GAPDH (Figs. 2 and 5). Additionally, GAPDH dimers can form distinct heterotetramers by associating with dimers of another enzyme [26,27]. Further, a docking model of the human WT-GAPDH dimer to a dimer of human C152A-GAPDH confirmed that this interaction is possible (Fig. 7B). These findings strongly indicate the formation of heterotetramer at equilibrium of the presence of each GAPDH tetramer, dimer, and monomer. Therefore, C152A-GAPDH might function as a dominant-negative molecule against both GAPDH aggregation and GAPDH-induced cell death through the formation of a heterotetramer with the aggregation-prone WT-GAPDH. This hypothesis provides a new potential therapeutic strategy for some neurological disorders related to GAPDH aggregation. In this regard, further *in vivo* study and analyses of the beneficial characteristics of C152A-GAPDH are needed. Currently, we have generated a conditional C152A-GAPDH transgenic mouse; this genetically modified mouse exerts robust neuroprotective effects on oxidative/nitrosative stress-triggered brain damage induced by middle cerebral artery occlusion (MCAO) in mice stroke model (unpublished data). Thus, the findings in this study, in particular the molecular mechanism underlying possible combating cell death utilizing by C152A-GAPDH, form the basis of therapeutic applications, in which we are investigating *in vivo*-study.

4. Conclusion

The present study shows that C152A-GAPDH acts as a dominant-negative mutant, protecting against GAPDH aggregation-induced cell death through the formation of the hybrid heterotetramer between GAPDH and C152A-GAPDH. This interference strategy may offer a novel insight into the therapeutic significance of mutant GAPDH in neurodegenerative/neuropsychiatric disorders that are accompanied by GAPDH aggregate formation.

Conflict of interest

The authors declare no conflict of interest.

Acknowledgments

We thank Drs. Andreas Pluckthun and Peter Lindner (Zurich University) for generously providing gap (−) *Escherichia coli* strain W3CG. This work was in part supported by the Japan Society for the Promotion of Science KAKENHI Grants (22580339 and 25450428) to H.N., and by grants from the Japan Science and Technology Agency for exploratory research in A-STEP: Adaptable and Seamless Technology Transfer Program through Target-driven R&D (AS232Z02185G and AS242Z02311Q) to H.N.

References

[1] M.R. Hara, M.B. Cascio, A. Sawa, GAPDH as a sensor of NO stress, Biochim. Biophys. Acta 1762 (2006) 502–509.
[2] A. Colell, D.R. Green, J.E. Ricci, Novel roles for GAPDH in cell death and carcinogenesis, Cell Death Differ. 16 (2009) 1573–1581.
[3] M.R. Hara, N. Agrawal, S.F. Kim, M.B. Cascio, M. Fujimuro, Y. Ozeki, M. Takahashi, J.H. Cheah, S.K. Tankou, L.D. Hester, C.D. Ferris, S.D. Hayward, S.H. Snyder, A. Sawa, S-nitrosylated GAPDH initiates apoptotic cell death by nuclear translocation following Siah1 binding, Nat. Cell Biol. 7 (2005) 665–674.
[4] N. Sen, M.R. Hara, M.D. Kornberg, M.B. Cascio, B.I. Bae, N. Shahani, B. Thomas, T.M. Dawson, V.L. Dawson, S.H. Snyder, A. Sawa, Nitric oxide-induced nuclear GAPDH activates p300/CBP and mediates apoptosis, Nat. Cell Biol. 10 (2008) 866–873.
[5] H. Nakajima, W. Amano, A. Fujita, A. Fukuhara, Y.T. Azuma, F. Hata, T. Inui, T. Takeuchi, The active site cysteine of the proapoptotic protein glyceraldehyde-3-phosphate dehydrogenase is essential in oxidative stress-induced aggregation and cell death, J. Biol. Chem. 282 (2007) 26562–26574.
[6] H. Nakajima, W. Amano, A. Fukuhara, T. Kubo, S. Misaki, Y.T. Azuma, T. Inui, T. Takeuchi, An aggregate-prone mutant of human glyceraldehyde-3-phosphate dehydrogenase augments oxidative stress-induced cell death in SH-SY5Y cells, Biochem. Biophys. Res. Commun. 390 (2009) 1066–1071.
[7] H. Nakajima, W. Amano, T. Kubo, A. Fukuhara, H. Ihara, Y.T. Azuma, H. Tajima, T. Inui, A. Sawa, T. Takeuchi, Glyceraldehyde-3-phosphate dehydrogenase aggregate formation participates in oxidative stress-induced cell death, J. Biol. Chem. 284 (2009) 34331–34341.
[8] C.A. Ross, M.A. Poirier, Protein aggregation and neurodegenerative disease, Nat. Med. 10 (Suppl) (2004) S10–S17.
[9] Q. Wang, R.L. Woltjer, P.J. Cimino, C. Pan, K.S. Montine, J. Zhang, T.J. Montine, Proteomic analysis of neurofibrillary tangles in Alzheimer disease identifies GAPDH as a detergent-insoluble paired helical filament tau binding protein, FASEB J. 19 (2005) 869–871.
[10] K. Tsuchiya, H. Tajima, T. Kuwae, T. Takeshima, T. Nakano, M. Tanaka, K. Sunaga, Y. Fukuhara, K. Nakashima, E. Ohama, H. Mochizuki, Y. Mizuno, N. Katsube, R. Ishitani, Pro-apoptotic protein glyceraldehyde-3-phosphate dehydrogenase promotes the formation of Lewy body-like inclusions, Eur. J. Neurosci. 21 (2005) 317–326.
[11] G.C. Brown, Nitric oxide and neuronal death, Nitric Oxide 23 (2010) 153–165.
[12] Z. Gu, T. Nakamura, S.A. Lipton, Redox reactions induced by nitrosative stress mediate protein misfolding and mitochondrial dysfunction in neurodegenerative diseases, Mol. Neurobiol. 41 (2010) 55–72.
[13] C.L. Avila, C.M. Torres-Bugeau, L.R. Barbosa, E.M. Sales, M.O. Ouidja, S.B. Socias, M.S. Celej, R. Raisman-Vozari, D. Papy-Garcia, R. Itri, R.N. Chehin, Structural characterization of heparin-induced glyceraldehyde-3-phosphate dehydrogenase protofibrils preventing alpha-synuclein oligomeric species toxicity, J. Biol. Chem. 289 (2014) 13838–13850.
[14] A. Pierce, H. Mirzaei, F. Muller, E. De Waal, A.B. Taylor, S. Leonard, H. Van Remmen, F. Regnier, A. Richardson, A. Chaudhuri, GAPDH is conformationally and functionally altered in association with oxidative stress in mouse models of amyotrophic lateral sclerosis, J. Mol. Biol. 382 (2008) 1195–1210.
[15] T. Nakamura, O.A. Prikhodko, E. Pirie, S. Nagar, M.W. Akhtar, C.K. Oh, S.R. McKercher, R. Ambasudhan, S.I. Okamoto, S.A. Lipton, Aberrant protein S-nitrosylation contributes to the pathophysiology of neurodegenerative diseases, Neurobiol. Dis. 84 (2015) 99–108.
[16] J.L. Jenkins, J.J. Tanner, High-resolution structure of human D-glyceraldehyde-3-phosphate dehydrogenase, Acta Crystallogr. D. Biol. Crystallogr. 62 (2006) 290–301.
[17] M.R. White, M.M. Khan, D. Deredge, C.R. Ross, R. Quintyn, B.E. Zucconi,

V.H. Wysocki, P.L. Wintrode, G.M. Wilson, E.D. Garcin, A dimer interface mutation in glyceraldehyde-3-phosphate dehydrogenase regulates its binding to AU-rich RNA, J. Biol. Chem. 290 (2015) 1770–1785.
[18] K. Suzuki, K. Hibino, K. Imahori, Hybridization of glyceraldehyde-3-phosphate dehydrogenase in borate, J. Biochem. 79 (1976) 1287–1295.
[19] K. Suzuki, M. Watanabe, K. Imahori, Glyceraldehyde-3-phosphate dehydrogenase of horseshoe crab (Tachypleus tridentatus), J. Biochem. 77 (1975) 269–279.
[20] N.K. Nagradova, Study of the properties of phosphorylating D-glyceraldehyde-3-phosphate dehydrogenase, Biochem. (Mosc) 66 (2001) 1067–1076.
[21] C. Ganter, A. Pluckthun, Glycine to alanine substitutions in helices of glyceraldehyde-3-phosphate dehydrogenase: effects on stability, Biochemistry 29 (1990) 9395–9402.
[22] H. Nakajima, T. Kubo, H. Ihara, T. Hikida, T. Danjo, M. Nakatsuji, N. Shahani, M. Itakura, Y. Ono, Y.T. Azuma, T. Inui, A. Kamiya, A. Sawa, T. Takeuchi, Nuclear-translocated glyceraldehyde-3-phosphate dehydrogenase promotes poly(ADP-ribose) polymerase-1 activation during oxidative/nitrosative stress in stroke, J. Biol. Chem. 290 (2015) 14493–14503.
[23] Y. Nekooki-Machida, M. Kurosawa, N. Nukina, K. Ito, T. Oda, M. Tanaka, Distinct conformations of in vitro and in vivo amyloids of huntingtin-exon1 show different cytotoxicity, Proc. Natl. Acad. Sci. U. S. A. 106 (2009) 9679–9684.
[24] B.G. Pierce, Y. Hourai, Z. Weng, Accelerating protein docking in ZDOCK using an advanced 3D convolution library, PLoS One 6 (2011) e24657.
[25] W.E. Klunk, R.F. Jacob, R.P. Mason, Quantifying amyloid by congo red spectral shift assay, Methods Enzymol. 309 (1999) 285–305.
[26] M. Engel, M. Seifert, B. Theisinger, U. Seyfert, C. Welter, Glyceraldehyde-3-phosphate dehydrogenase and Nm23-H1/nucleoside diphosphate kinase A. Two old enzymes combine for the novel Nm23 protein phosphotransferase function, J. Biol. Chem. 273 (1998) 20058–20065.
[27] F. Mouche, B. Gontero, I. Callebaut, J.P. Mornon, N. Boisset, Striking conformational change suspected within the phosphoribulokinase dimer induced by interaction with GAPDH, J. Biol. Chem. 277 (2002) 6743–6749.